

A Fundamental Investigation of the Formation and Properties of Electrospun Fibers

G.C. Rutledge, M.Y. Shin

*Departments of Chemical Engineering and Materials Science and Engineering,
Massachusetts Institute of Technology, Cambridge, MA 02139*

S.B. Warner, A. Buer, M. Grimler, S.C. Ugbolue

*Department of Textile Sciences, University of Massachusetts Dartmouth,
Dartmouth, MA 02747*

Abstract and Objectives

The objective of this project is the development of the fundamental engineering science and technology of electrostatic fiber production (“electrospinning”). Electrospinning offers unique capabilities for producing novel synthetic fibers of unusually small diameter and good mechanical performance (“nanofibers”), and fabrics with controllable pore structure and high surface area. The project aims to achieve the following goals:

1. Design and construction of process equipment for controllable and reproducible electrospinning.
2. Clarification of the fundamental electrohydrodynamics of the electrospinning process and correlation to the polymer fluid characteristics.
3. Characterization and evaluation of the fluid instabilities postulated to be crucial for producing ultrafine diameter fibers.
4. Characterization of the morphology and material properties of electrospun polymer fibers.
5. Development of techniques for generating oriented fibers and yarns by the electrospinning process.
6. Productivity improvement of the electrospinning process.

Introduction

Conventional fiber spinning techniques, e.g. melt spinning, dry spinning or wet spinning, rely on mechanical forces to produce fibers by extruding polymer melt or solution through a spinnerette and subsequently draw the resulting filaments as they solidify or coagulate. Electrospinning offers a fundamentally different approach to fiber production by introducing electrostatic forces to modify the fiber formation process. Although the idea goes back at least 60 years [1], exploitation of technologies based on electrospinning have been very limited, due to poor understanding of the process and consequent limitation in process control, reproducibility and productivity. Interest has renewed in recent years with the work of Reneker and co-workers, who have demonstrated electrospinning for a wide variety of materials and solutions [2,3] and have produced a number of different and interesting fiber structures and morphologies [3-5]. Notable among these are fiber of extremely small diameters (40 nm in the case of electrospun poly(p-phenylene terethalamide), or Kevlar, fibers) [3] and “beaded” fibers [6,7]. Larrondo and Manley were the first to demonstrate electrospinning of polyethylene and polypropylene fibers from the melt [8,9]. Permeability studies on electrospun fabrics indicate potential for membrane and filtration applications [10]. Electrospun fabrics have

also been shown to impart some improved mechanical performance characteristics in rubber and epoxy matrix composites [11].

The basic process of electrospinning involves the introduction of electrostatic charge to a stream of polymer melt or solution in the presence of a strong electric field. The predominant form of operation entails charge induction in the fluid through contact with a high voltage electrode in a simple metal or glass capillary spinnerette. A charged jet is produced which accelerates and thins in the electric field, ultimately collecting on a grounded device, typically a plate or belt. Under certain conditions of operation, the fluid jet becomes unstable before it reaches the collector. With low molecular weight fluids, the onset of instability typically results in a spray of small, charged droplets, in a process known as "electrospraying". With polymeric fluids, viscoelastic forces stabilize the jet, permitting the formation of small diameter, charged filaments that appear as an "envelope" or cone of dispersed fluid, and that solidify and deposit on the collector in the form of a nonwoven fabric. Under these conditions, it is common to observe mean fiber diameters on the order of 0.1 μm , three orders of magnitude smaller than the diameter of the jet entering the unstable region (100 μm), and well below the diameter of conventional extruded fibers (10-100 μm). We [12-15] and others [16,17] have shown that the dominant mechanism responsible for the instability cone and subsequent diameter reduction is a whipping mode instability. Other modes of instability, such as splitting [2-4], are also observed on occasion.

Experimental

1. Equipment Design

Electrospinning equipment has been fabricated at both sites collaborating on this proposal, University of Massachusetts at Dartmouth (UMD) and Massachusetts Institute of Technology (MIT). In addition to conventional test equipment consisting of simple fluid reservoirs connected to a high voltage power supply, specialized designs have also been constructed for the purposes of (a) studying simple electrohydrodynamic flows amenable to mathematical analysis (MIT) and (b) investigating methods for increasing the productivity of electrospinning (UMD).

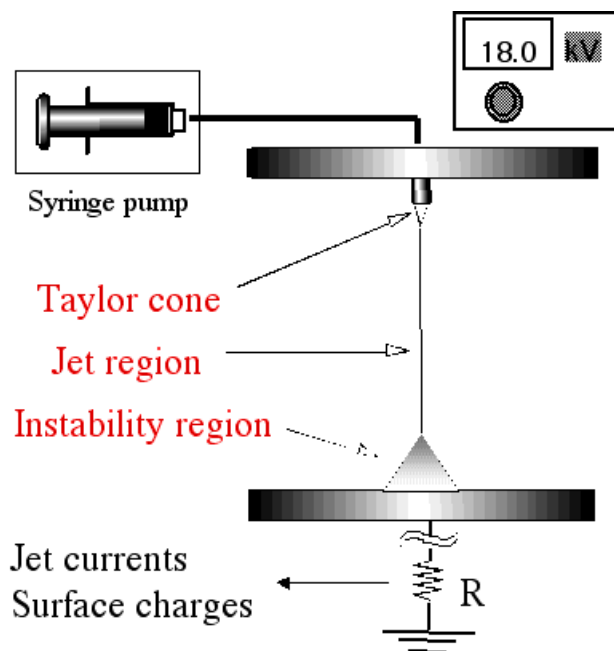


Figure 1. Instrumented electrostatic spinner design with parallel-plate geometry

The electrospinner design used for study of electrohydrodynamic flows is illustrated in Figure 1. In particular, flow rate is controlled using a digitally controlled, positive displacement syringe pump (Harvard Apparatus PHD 2000, flow rates: 0.0001 $\mu\text{l/hr}$ – 220 ml/min) which delivers fluid to the spinnerette via flexible Teflon tubing. The spinnerette is a stainless steel tube with outer diameter of 0.0625 inch and an inner diameter of 0.04 in. Applied voltage is regulated up to 30 kV using a Gamma High Voltage Research ES30-P power supply. Lastly, electric field equations are simplified by implementing a parallel-plate electrospinner design, as shown in Figure 1, although the experiments were run both with and without the top plate in place. By adjusting the protrusion of the spinnerette tip from the upper plate, we can vary the electric field curvature near the spinnerette, independent of other parameters. Typical operating regimes are flow rates between 0.2 and 2 ml/min, voltages between 10 and 20 kV, and spinnerette-to-collector distance of 10 to 20 cm. The parallel plates are 10 cm aluminum disks.

During the course of this project, two avenues of productivity enhancement have been pursued (UMD). The first of these involves scale-up through use of multiple spinnerettes (a "rotorspinner") [12]. Such designs are complicated, however, by electrostatic interference between spinnerettes, due to the long range nature of electrostatic interactions. The second approach followed involves alternate methods for charging the fluid. While most current electrospinning implementations rely on some combination of induction charging and frictional charging to transfer charge from electrode to fluid, other methods based on plasma charging and direct charge injection may offer the opportunity to couple charging of the fluid to different fluid and electrode parameters. With this latter configuration, flow rates on the order of 50 ml/s, several orders of magnitude higher than current induction configurations, may be possible.

2. Fluids

A wide range of fluids can be spun by the electrospinning technique. However, the UMD/MIT team has focused on a few model systems for performing its fundamental investigations. At MIT, glycerol has been used to clarify the fundamental electrohydrodynamic behavior of the jet. Viscosity, permittivity and conductivity are variable over a wide range by mixing glycerol with water. Glycerol and glycerol/water mixtures are well-characterized, miscible Newtonian fluids. Solutions of polyethylene oxide (PEO) in water and PEO in chloroform are also used. KBr is used to vary the conductivity of these solutions. At UMD, PEO in 6:1 isopropanol:water and polyacrylonitrile (PAN) in dimethylformamide (DMF) have been spun. The use of isopropanol mixed with water allows modification of both the conductivity and evaporation rate of the spin dopes. Standardized solutions based on PEO/water facilitate comparison of experimental results with results in the literature as well as between the MIT and UMD groups.

3. Characterization methods

Quantitative analysis of the electrospinning process falls into four categories. These are described in detail in a previous report [12] and consist of the following:

- (1) *Solution properties.* The relevant fluid properties are density, viscosity, surface tension, permittivity, conductivity and viscoelasticity. Of these, viscosity and conductivity appear to play the greatest role in the electrospinning of dilute solutions. For all the electrohydrodynamic modeling studies, the solutions used were confirmed to be non-shear-thinning for the range of wall shear rates expected to occur in the spinnerette.
- (2) *Operating parameters.* The relevant operating parameters are flow rate, electric field strength, and electric current flow between the spinnerette and collector. The volumetric flow rate is closely controlled through the use of the syringe pump. Field strength may be varied by changing either the applied voltage or the distance over which the voltage drop to ground occurs. Both variables have been studied. Thinning of the jet depends principally on the field strength; however, the development of instabilities in the jet requires sufficient distance of travel for the instabilities to grow in amplitude. The total electric current contains contributions from both convection and conduction currents, and provides an indirect measure of the total surface charge density on the jet. Surface charge density, in turn, is believed to play a major role in determining jet stability. Jet current is measured by monitoring the voltage drop across a resistor between the collector and ground, and correcting for any displacement current between the parallel plates.
- (3) *Online process monitoring.* Macrophotography is used to image the thinning of the fluid jet as it leaves the spinnerette. For this purpose, we use a long distance microscopy or extension tubes connected to a conventional 35 mm camera, providing magnification of 10x or higher. Area backlighting is used for highest contrast and resolution of the jet. IDL software is used for image analysis. Strobe photography is used to study the instability in the jet. A continuous pulse (GenRad 1538A) strobe is used to monitor the instability continuously. A Nanolite II high intensity strobe with a 20 ns pulse length is used to capture the instabilities on film. The high intensity strobe is arranged to backlight the fluid stream, for highest resolution. A Dantec LDA EduSys 3 system, designed for forward scatter operation and fitted with 10 mW coaxial He-Ne laser and wavelength of 632 nm has been used to perform laser Doppler velocimetry measurements.

- (4) *Fiber characterization.* Fiber diameter distributions are measured using scanning electron microscopy. Samples of nonwoven webs were coated with gold-palladium using a Denton Vacuum Desk II sputtering machine and observed using an AMRAY 1200B SEM. Fiber diameters were sampled by measuring the width of those fibers intersected by a straight line drawn at random across the image. Fibers were also observed using a Leica DMRX polarized optical microscopy with Sernamount compensator, green filter (546 nm) and Zeiss Microfilar Microcode eyepiece. Fibers were observed in a mounting liquid with refractive index 1.546. Single fiber tenacity has been measured using a cantilever technique, described in detail elsewhere [12].

Mathematical modeling

In collaboration with M.P. Brenner (Department of Mathematics, MIT) and M. Hohman (James Franck Institute, University of Chicago) a mathematical model of the electrospinning process has been developed for Newtonian fluids. The model invokes an asymptotic expansion in jet radius in order to simplify the full set of electrohydrodynamic equations for a long, slender jet, but retains validity for fluids with representative conductivities, viscosities, charge densities, etc. From the jet profile and surface charge distribution predicted by the thinning jet model, linear stability analyses are possible which predict the growth rates of several axisymmetric (“varicose”) and non-axisymmetric (“whipping”) instabilities. A detailed analysis of these instabilities and their dependence on fluid properties and operating parameters permits a near-quantitative comparison between theory and experiment that offers compelling evidence for the validity of the mathematical model.

Results

The experimental results for studies of model fluids glycerol and PEO/water solutions have recently been reported elsewhere in the technical literature [18]. Representative highlights of this work are summarized here.

Jet Profiles. Jet profiles provide a remarkable record of the transition from pressure-driven flow to electrically-driven flow. Figure 2 illustrates three jet profiles for glycerol obtained at a fixed flow rate (0.5 ml/min) under different applied field strengths (3.67-5 kV/cm). The change of shape of the Taylor cone from convex to concave is in accord with changes in charge density as the field strength is varied. However, the thinning jet is relatively insensitive to the details of the Taylor cone; all three jets are very similar in diameter after proceeding a distance equal to only 2-3 nozzle radii downstream. The reasons for this, and subsequent modeling efforts to understand the development of flow in the nozzle regime, are explained in greater detail in the related NTC-sponsored project, M01-D22 [19].

For Newtonian fluids, the jet thinning scales as

$$r \propto z^{-1/4}$$

where r is the jet radius and z is the axial distance from the nozzle. This is in accord with previous analyses [20,21]. After allowance is made for image charges and field line curvature at the spinnerette, quantitative agreement with experimental observations for glycerol is obtained, as illustrated in Figure 3.

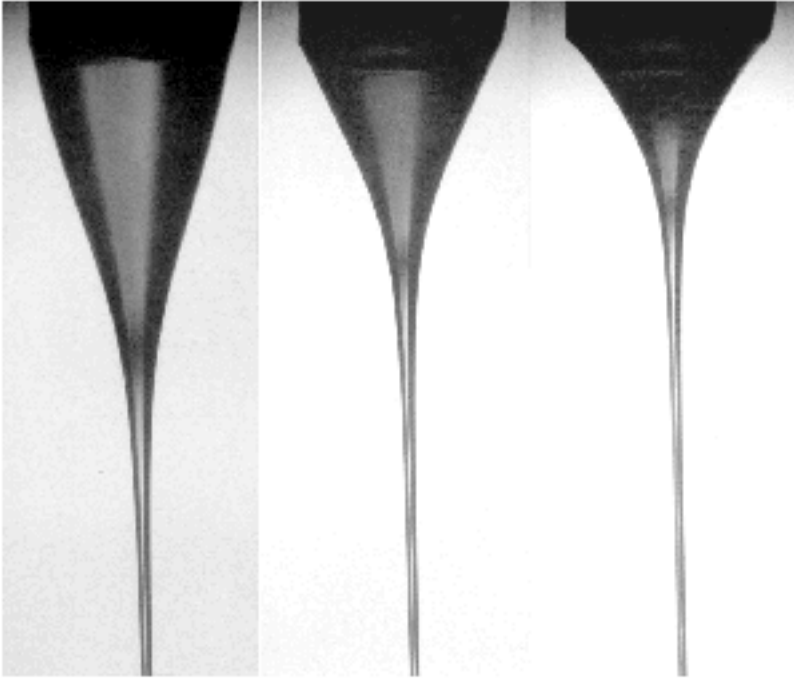


Figure 2. Glycerol jets at 0.5 ml/min. Left to right: 3.67 kV/cm, 4.33 kV/cm, 5.0 kV/cm.

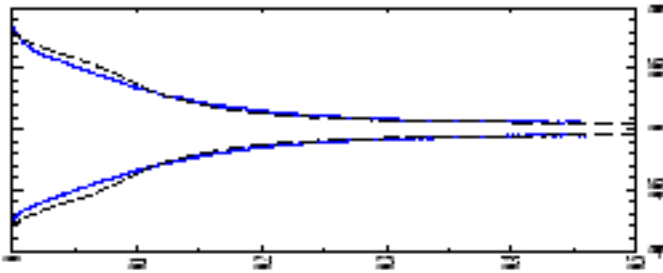


Figure 3: Comparison of experimental and theoretical jet profiles for glycerol. Nozzle diameter 0.794 mm, protruding 7.2 mm from top plate. Flow rate = 1.5 ml/min, electric field = 5.0 kV/cm. Solid lines: experimental measurement by macrophotography; dashed lines: theoretical prediction. Image rotated by 90 degrees.

Whipping instability. Using high speed photography, we have imaged the onset of instabilities in glycerol and PEO/water jets (2,000,000 MW PEO) (i.e. the apex region of the “inverted cone” shown in Figure 1). Depending on fluid properties and operating conditions, both varicose and whipping instabilities have been observed and imaged. We have found the instabilities to behave as convected phenomena; thus, each mode may grow at a different rate, dependent on jet radius and surface charge density, and a single jet may exhibit more than one mode of instability. Of particular importance, the mathematical model suggests that varicose instabilities may arise due to either surface tension or electrostatic forces. The whipping instability, on the other hand, arises solely

due to electrostatic forces. Both mutual charge repulsion and interactions of dipolar fluctuations in the surface charge distribution are important causes of the bending instability. By varying the concentration of salts in glycerol, we have observed both varicose and whipping instabilities in this model Newtonian fluid. The onset of whipping instability occurs when the conductivity of the fluid is high enough to allow induction of high charge densities in the fluid. An example of an operating diagram for a glycerol/KBR solution which exhibits whipping is shown in Fig. 4. PEO/water solutions also exhibit both varicose and bending instabilities, consistent with the high conductivity of water.

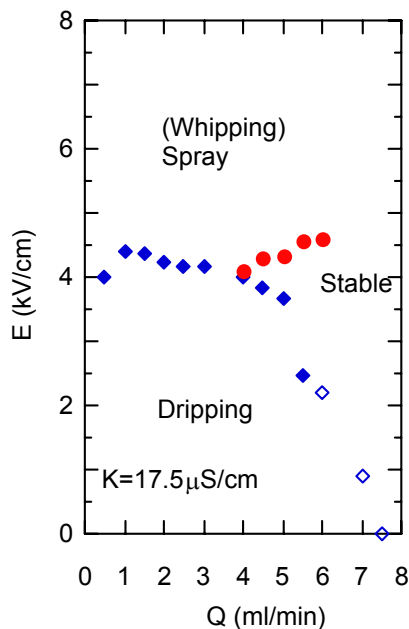


Figure 4: Operating Diagram for glycerol/KBr solution, showing three regimes of operation previously found for PEO/water solutions.

Charge density Jet currents have been measured as functions of flow rate and applied field strengths for several model fluids characterized by different conductivities. Over a wide range of field strengths, the current is linearly dependent on flow rate. From the ratio of current to flow rate, an indication the charge density induced for a given field strength can be obtained. This is illustrated in Figure 5 for solutions of PEO/water measured under steady jet operation at fields between 0.5 and 2.0 kV/cm. For PEO/water solutions, the charge density varies from about 0.3 to 1.5 mC/cm³.

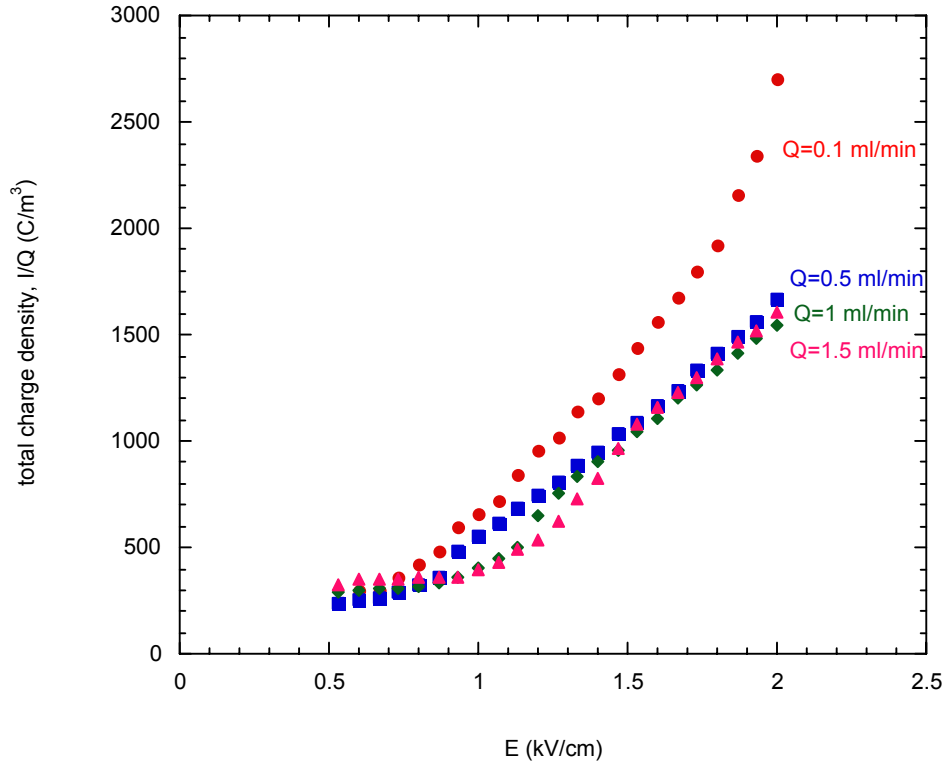


Figure 5. Charge density (computed as the ratio of electric current to flow rate, I/Q) for steady jets of PEO/water.

Conclusion and Outlook

We believe we now have a working description of the electrohydrodynamic behavior of fluid jets under conventional electrospinning operation, extending from the spinnerette to the onset of instability [13-15,18]. The key process parameters and material properties that control process operation have been identified and operating diagrams proposed to classify regimes of operation. In collaboration with mathematicians, a model has been developed which accords with our experimental observations of jet thinning, jet current, and regimes of operation.

Acknowledgements

The authors are grateful to the National Textile Rcenter for financial support of this project, under US. Department of Commerce Grant 99-27-7400.

Web site: <http://heavenly.mit.edu/~rutledge/electrospin.html>

References

- [1] A. Formhals, US Patent 1,975,504 (1934)
- [2] G. Srinivasan, D.H. Reneker, *Polym. Int.*, 36, 195 (1996).
- [3] D.H. Reneker, I. Chun, *Nanotechnology*, 7, 216 (1996).
- [4] J. Doshi, D.H. Reneker, *J. Electrostatics*, 35, 151 (1995).
- [5] H. Fong, I. Chun, D.H. Reneker, *Polymer*, 40, 4585 (1999).
- [6] H. Fong, D.H. Reneker, *J. Polym. Sci.-Phys.*, 37, 3488 (1999).
- [7] R. Jaeger, M.M. Bergshoef, C. Martin-I-Batlle, D. Schoenherr, G.J. Vancso, *Macromol. Symp.*, 127, 141 (1998).
- [8] L. Larrondo, R. St. John Manley, *J. Polym. Sci. – Phys.*, 19, 909, (1981).
- [9] L. Larrondo, R. St. John Manley, *J. Polym. Sci. – Phys.*, 19, 921, (1981).
- [10] P.W. Gibson, H.L. Schreuder-Gibson, D. Rivin, *AIChE J.*, 45, 190 (1999).
- [11] J.-S. Kim, D.H. Reneker, *Polymer Comp.*, 20, 124 (1999).
- [12] S.B. Warner, A. Buer, M. Grimler, S.C. Ugbolue, G.C. Rutledge, M.Y. Shin, *NTC Annual Report, Project M98-D01* (1999).
- [13] M.Y. Shin, M.M. Hohman, M. Brenner and G.C. Rutledge, *Appl. Phys. Lett.* 78, 1149 (2001).
- [14] M.M. Hohman, Y.M. Shin, G. Rutledge and M.P. Brenner, *Phys. Fluids* 13, 2201 (2001).
- [15] M.M. Hohman, Y.M. Shin, G. Rutledge and M.P. Brenner, *Phys. Fluids* 13, 2221 (2001).
- [16] D.H. Reneker, A.L. Yarin, H. Fong and S. Koombhongse, *J. Appl. Phys.* 87, 4531 (2000).
- [17] A.L. Yarin, S. Koombhongse and D.H. Reneker, *J. Appl. Phys.* 89, 3018 (2001).
- [18] Y.M. Shin, M.M. Hohman, M.P. Brenner and G.C. Rutledge, *Polymer*, 42, 9955 (2001).
- [19] G.C. Rutledge, Y. Li, S. Fridrikh, S.B. Waner, V.E. Kalayci, and P. Patra, *NTC Annual Report M01-D22* (2001).
- [20] V.N. Kirichenko, I.V. Petryannov-sokolov, N.N. Suprun, A.A. Shutov, *Sov. Phys. Dokl.*, 31, 611, 1986.
- [21] A.M. Ganan-Calvo, *Phys. Rev. Lett.*, 79, 217 (1997).